Efficient Deep Blue Organic Light-Emitting Diodes Based on Thermally Activated Delayed Fluorescence Emitter with Simplified Device Structure

Leijuan Ma, Jinglin Xu, Mingjian Zhang, Qi zhu*

Henan Polytechnic Institute, Nanyang, China

*Corresponding Author's Email: qzhu@mails.cust.edu.cn

Abstract: In this study, we have designed a series of blue electroluminescent (EL) devices with streamlined structures based on conventional electron transport materials. The incorporation of TcTa layer leads to a distinct improvement in the EL properties, which is attributable to the balanced distribution of the charge carriers and the extent of the recombination zones in the emission layer. In addition, it has been found that the auxiliary thickness of the stepwise TcTa layer is advantageous in order to improve the color purity of the device. Finally, device obtained the highest brightness, current efficiency, power efficiency, power efficiency and external quantum efficiency (EQE), reaching 3914 cd/m²,12.58 cd/A, 12.69 lm/W and 13.1% respectively. The color coordinates of the device are (0.176, 0.159), which are shown in dark blue..

Keywords: electroluminescence; TADF material; Dark blue; Step by step levels

1. Introduction

Organic light-emitting diodes (OLEDs) have attracted the attention of researchers for decades because of their potential applications in solid-state lighting and full-color displays[1-5]. Compared to green and red materials, blue emitters often exhibit suboptimal performance, resulting in lower device efficiency, shortened device life, and compromised color purity[6-8]. Developing efficient and stable blue devices is a major challenge for the advancement of OLED technology[9-12]. Due to the large forbidden bandwidth of the blue emitter, it is relatively easy to cause excitation energy to be too high, which can lead to exciton-exciton interactions or exciton-polarizer interactions that destroy the chemical structure of the molecule[14,15]. This will have a significant impact on the efficiency and lifespan of blue devices[16]. The choice of material with a narrow bandwidth is not enough to meet a high color rendering index[17]. Designing more efficient and stable blue emitters is a crucial step in overcoming the challenges associated with OLED materials.

To meet this need, purely aromatic thermally activated delayed fluorescence materials (TADF) were prepared. Zhang et al [18]. designed a blue TADF emitter material, bis [4-(9, 9-dimethyl-9, 10-dihydroacridine) phenyl] sulfone (DMAC-DPS), which exhibits a distorted molecular configuration and significantly inhibits intramolecular charge transfer. The HOMO and LUMO levels are highly separated and promote a small Δ E_{ST} for effective RISC progression. In addition, DMAC-DPS-based OLEDs have a high external quantum efficiency (EQE) of 19.5% and international lattice coordinates (CIE) of (0.16, 0.20). Kim et al [19]. designed and constructed two sky blue TADF transmitters, DCZTRZ and DDCZTRZ. Blue OLEDs based on these two emitters emit 459 and 459 respectively. 467 nm, which has a longer lifetime than blue phosphorescent OLEDs based on Ir (dbi)₃. Although new materials improve the performance of devices, few studies have been conducted to optimize the structural design of devices.

The aim of this study is to propose a strategy to improve the performance of the CZ-PS by designing a simplified device structure. The electron transport material Tm3PyP26PyB was used as the host material to simplify the device structure, and a TcTa layer was inserted as a stepwise intermediate layer between HTL and EML to achieve a balance between injection and pore transport. By optimizing the doping concentration of the emitter and the thickness of the deposited layer, a dark blue device with maximum current efficiency and external quantum efficiency (EQE) of 13.63 cd/A and 13.1%, respectively, was obtained.

2. Methodology

All organic materials used in this investigation were sourced from Luminescent Technologies and were used in their original state without any cleaning. The anode substrate consists of indium tin oxide (ITO) coated glass with a disk resistance of $10~\Omega/sq$. The patterned ITO substrate is washed with a detergent before film deposition, rinsed in deionized water and finally dried in an oven. The organic layer is deposited in a high vacuum. It is prepared by co-evaporation of CZ-PS with host

materials from two sources, and the doping concentration is adjusted by controlling the evaporation rate of CZ-PS. MoO₃, lithium fluoride and Al in another vacuum chamber at velocities of 0.01, 0.01 or 1 nm/s and without atmospheric action. The thickness of the deposited layers and the evaporation rate of the individual materials were monitored under vacuum with a quartz crystal monitor. On any substrate. The current density-brightness-voltage characteristics (J-B-V) were measured with programmable Keith light source measuring units (Keithley 2400 and 2000). The EL spectra were measured with a calibrated Hitachi F-7000 fluorescence spectrophotometer. From the light energy measured by the photodiode, the EL spectrum and the current flowing through the device, the external quantum efficiency (EQE) of the device was calculated. CIE1931 Standard Method for Chromatic Coordinates.

3. Results and discussion

Figure 1 shows the energy level diagram and molecular structure of the optimized devices for CZ-PS, TcTa and Tm3PyP26PyB .In this case, the MoO3 use to inject the intermediate material and inoculate the hole [20-22]. Di-4 (N, N-diolaminophenyl) cyclohexane (TAPC) was selected as the hole transport layer (HTL) and as the electron blocking layer (EBL). CZ-PS was chosen as the emitter because of its pure blue emission (peak in toluene at 404 nm wavelength) and the great separation of the Homound and Lumo mirrors. Tm3PyP26PyB was selected as the electron transport layer and as the main film because of its high electron mobility [23-27].

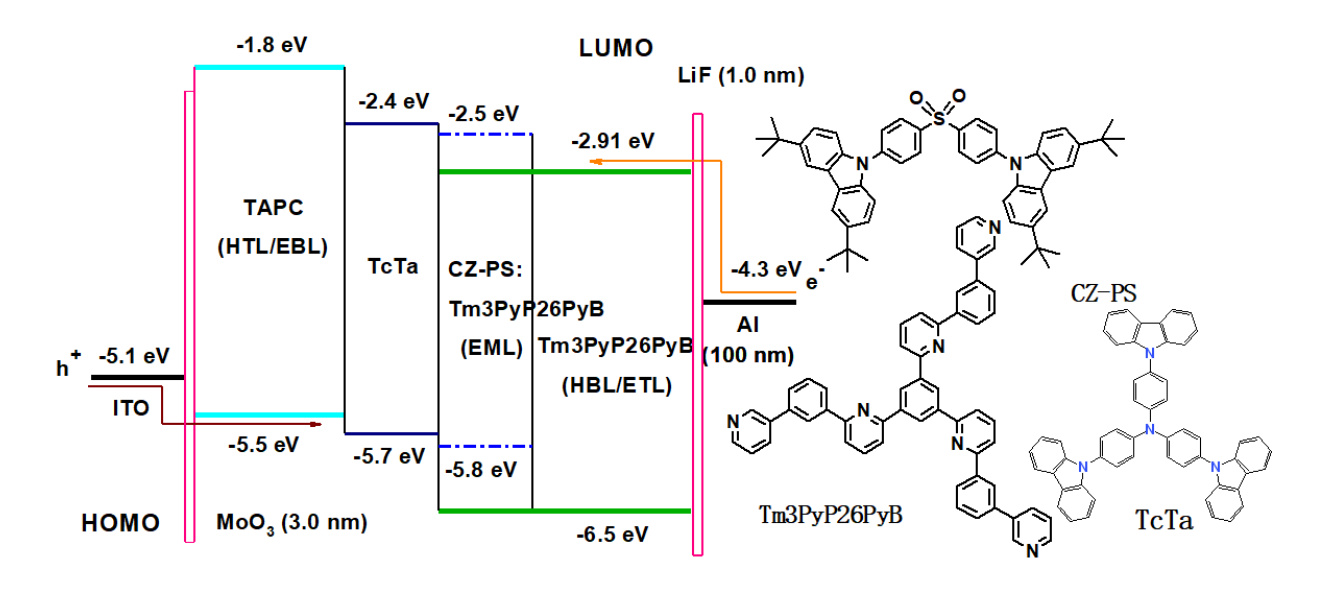


Fig. 1. Energy levels of the devices in this work and the molecular structures.

Initially, a series of devices were produced. The detailed performances of these examples are shown in Figure 2 (a). The experimental results show that at 5 a doping concentration of 10% by weight a maximum brightness of 1854 cd/m², a current efficiency of 11.68 cd/A, a power efficiency of 11.76 lm/W and an EQE of 11.3% are obtained. Switching-on voltage shows the normalized EL spectra of these devices in Figure 2(b), which operate at a current density of 10 mA/cm2. The EL spectrum of 10% by weight has a peak of 463 nm and the CIE coordinates of (0.178, 0.164). Furthermore, at approx. 575 nm a further emission peak originating from excimers is observed [28–30].

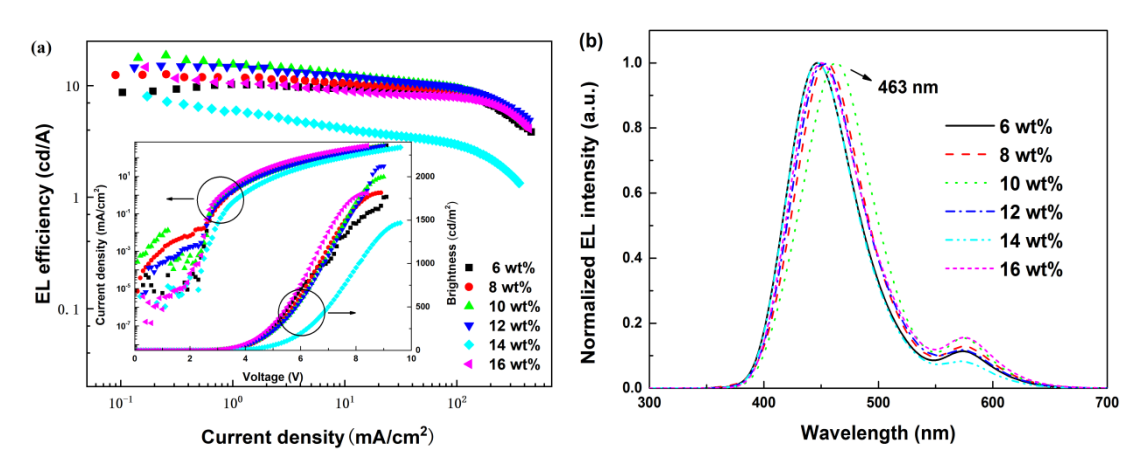


Fig. 2. (a) EL efficiency-current density characteristics of single-EML devices. (b) EL spectra of the single-EML devices at 10 mA cm⁻².

For comparison, we have produced another series of dual EML devices, which are structured as follows: ITO/MoO3(3 nm)/TAPC (50 nm)/CZ-PS (x% by weight): TAPC (10 nm)/CZ-PS (x% by weight): Tm3PyP26PyB (10 nm)/Tm3PyP26PyB (50 nm)/LiF (1 nm)/Al (100 nm). The values for x are given as 6, 8, 10, 12, 14 and 16, respectively. Figure 3 (a) show detailed EL performance data. The 10% doped devices have the highest brightness, current efficiency, power efficiency and EQE of 1853 cd/m², 12.21 cd/A, 12.39 lm/W and 11.5%, respectively. Compared to single EML devices, dual EML devices have reduced brightness but improved EL efficiency. The presence of double EMLs reduces the barriers to hole transport and thereby facilitates the hole injection of HTL into EML, thereby improving the balance of holes and electrons on the Cz-PS molecule. Figure 3 (b) shows the normalized EL spectra of dual EML devices, which show purer blue emission than single EML devices.

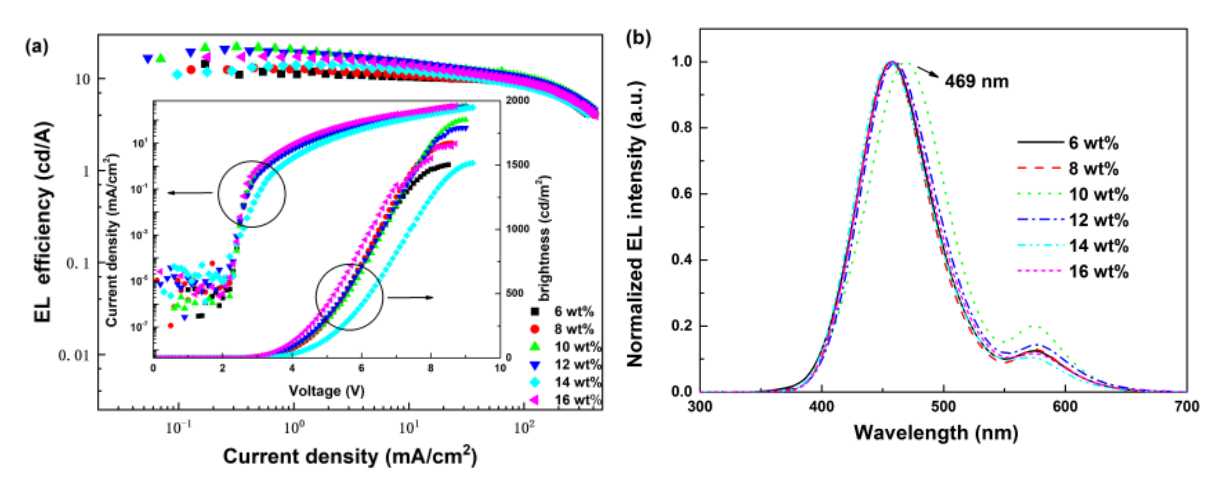


Fig. 3. (a) EL efficiency-current density of the double-EMLs devices. (b) EL spectra of the double-EMLs devices at 10 mA cm⁻².

As shown in Figure 3 (a), the EL efficiency of dual EML devices is lower than that of single EML devices at high current densities. At a brightness of 1000 cd/m², the efficiency of a single EML device decreases more slowly than a dual EML device. 6 Therefore, single EML devices show superior EL performance and greater ease of use compared to dual EML devices. To improve the performance of the EL, a TcTa thin layer was successively inserted between the HTL and the EML. This stepwise layer facilitates the transport of holes, resulting in a balanced distribution of electrons and holes and a wider recombination range. In addition, the performance of the EL has improved in terms of both brightness and efficiency, as shown in the Figure. 4 (a). Finally, devices with showed the highest brightness (3864 cd/m²), current efficiency (12.58 cd/A), power efficiency (12.69 lm/W) and EQE (13.0%). This study shows that adding TcTa layers to these devices can significantly improve their EL performance by up to 50%.

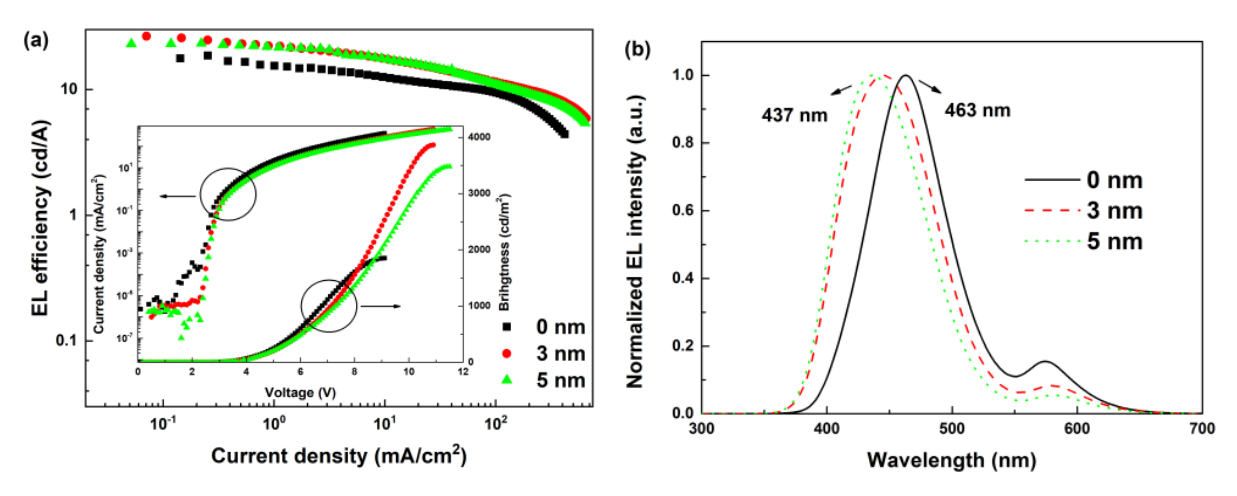


Fig. 4. (a) EL efficiency-current density of the devices with TcTa at different thicknesses. (b) EL spectra of the devices with TcTa layer at different thicknesses.

It is suspected that the key to achieving high EL performance in these devices is to try to efficiently regulate the injection and transport of holes, leading to a more balanced distribution of charge carriers across the emitter molecules. In addition, the EL spectrum of the single EML device with 5 nm without TCTA layer shows a clear blue shift of approximately 26 nm, as in Figure 4 (b). The inclusion of the TcTa layer significantly improves EL performance, along with a reduction in emission energy loss, blue shift and excimer peak reduction. This shows that the device structure for the emitter is advantageous to use excitons for light emission and improve the purity of blue emission. This gives a dark blue CIE (0.163, 0.088). Once the frame of the device is built up, the thickness of the ETL is further optimized. As shown in the Figure 5 (a), the highest brightness for the 7 device with an ETL thickness of 60 nm (3914 cd/m2), current efficiency (13.63 cd/A), power efficiency (13.56 lm/W) and EQE (13.1%).

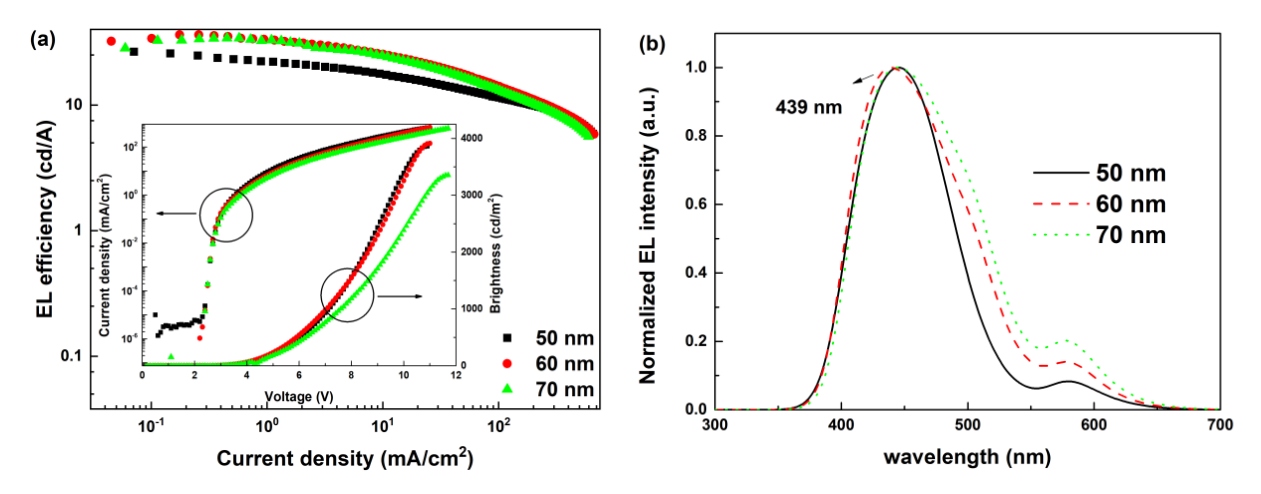


Fig. 5. (a) EL efficiency-current density of devices with electron transport layer at different thicknesses. EL spectra of devices with electron transport layer at different thicknesses.

As shown in Figure. 5 (b), the normalized EL spectral peak is at 439 nm. We hypothesize that the widened ETL promotes electron injection into the EML and thereby balances the distribution of electrons and holes within the EML. This in turn leads to a certain pore accumulation in EML, which counteracts the initial pore defects and ultimately leads to an improvement in EL performance. We then constructed devices with the following structure: ITO/MoO3 (3 nm)/TAPC (y nm) (y = 40, 45, 50, 50, 50, 50, 60)/TcTa (3 nm)/CZ-PS (10%): Tm3PyP26PyB (10 nm)/Tm3 PyP26PyB (60 nm)/LiF (1 nm)/Al (100 nm) was prepared to determine the thickness of the HTL.

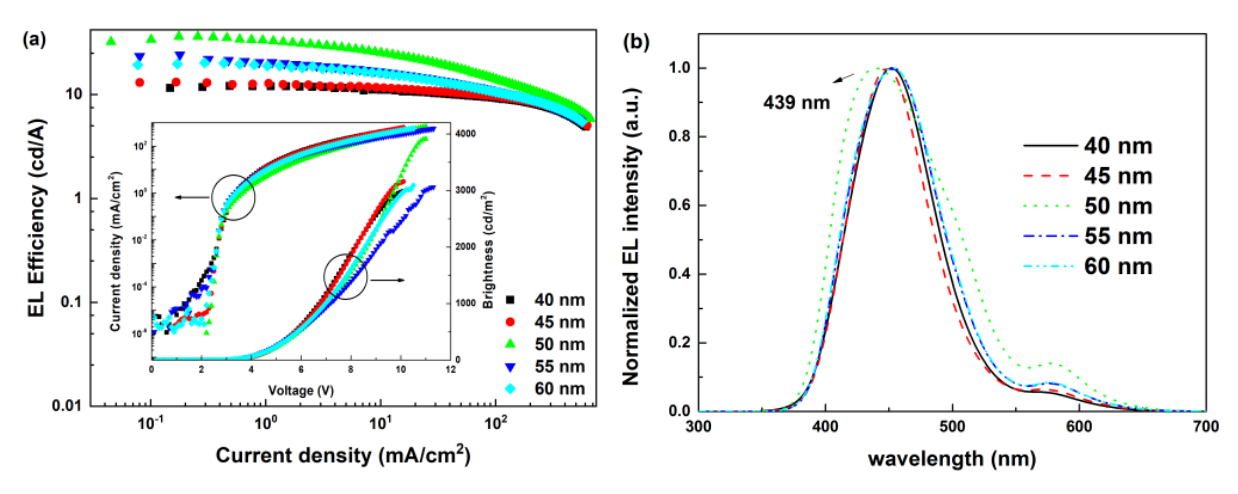


Fig. 6. (a) EL efficiency-current density of devices with hole transport layer at different thicknesses. (b) EL spectra of devices with hole transport layer at different thicknesses.

The EL properties of these devices are shown in Figure 6 (a), Figure 6 (b). The optimized HTL thickness is 50 nm, identical to previous optimizations. This suggests that in this case, 50 nm is the optimal thickness for HTL to achieve efficient hole transport. In addition, it shows that the key to achieving devices with high EL performance is to effectively control the implantation and transport of holes. At the same time, we try to optimize the thickness of EML. The detailed EL performances of the designed devices with different EML thicknesses are shown in Figure 7(a), and (b), respectively. Remarkably, the EL performance of devices with 10 nm EML shows an encouraging improvement compared to devices with EML thicknesses of 6 and 8 nm. This shows that the extension of the EML helps to achieve high EL efficiency and color purity. To gain a deeper understanding of the mechanism of the improved EL efficiency of 8 these devices, the distribution of holes and electrons in these devices is also analyzed.

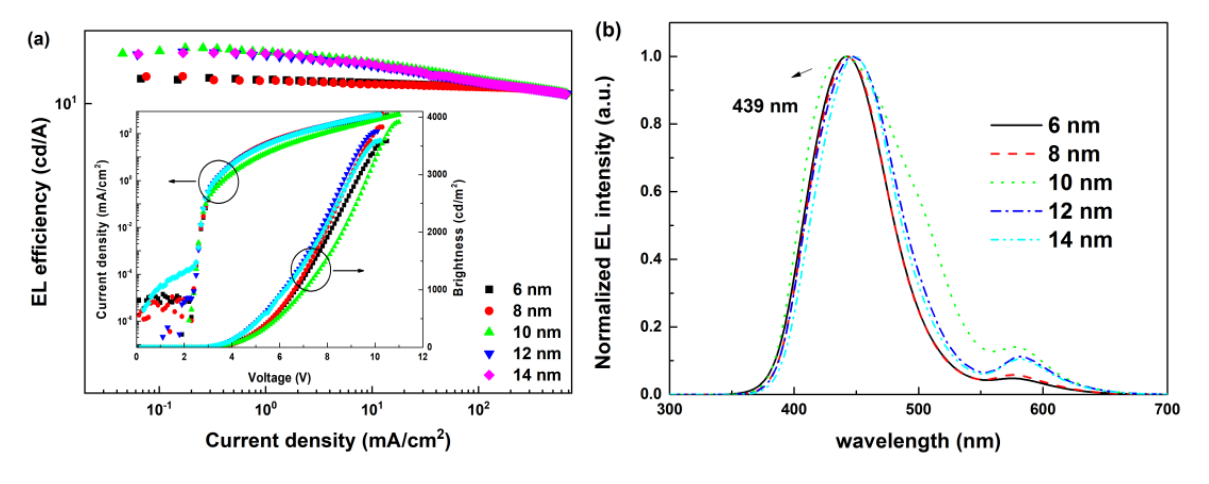


Fig. 7. (a) EL efficiency-current density of devices with emitting layer at different thicknesses. (b) EL spectra of the devices with emitting layer at different thicknesses.

As shown in Figure 8, device (a), the electrons are localized on the CZ-PS molecule due to the efficient electron transport properties of the host material Tm3PyP26PyB. On the contrary, due to the high pore blocking ability of Tm3PyP26PyB, pores accumulate in the TAPC layer near the interface between TAPC and EML. In the device (b), the insertion of the TcTa layer facilitates the implantation of the holes in the EML. At the same time, the TcTa layer also balances some electrons on CZ-PS, improving the balance of holes and electrons on CZ-PS molecules. Accordingly, device (b) exhibits improved EL performance and blue shift of the EL spectrum, indicating superior color purity. The device (c) has a thicker ETL layer compared to (b). With increasing ETL thickness, electron transport is delayed. Theoretically, increasing the implantation rate of pores contributes to the formation of a recombination region near ETL, which is advantageous for maintaining the balance of charge carriers on the CZ-PS molecule and expanding the recombination region. The device (b) thus exhibits the purest CZ-PS emission, while the device (c) in this case achieves the highest EL efficiency. It can be seen that the design of the device structure with electron transport materials as the main body and step-by-step energy levels of injection and transport of holes is

advantageous, balancing the distribution of charge carriers and even improving the trapping ability of charge carriers. This reduces the operating voltage and improves EL efficiency, brightness and color purity.

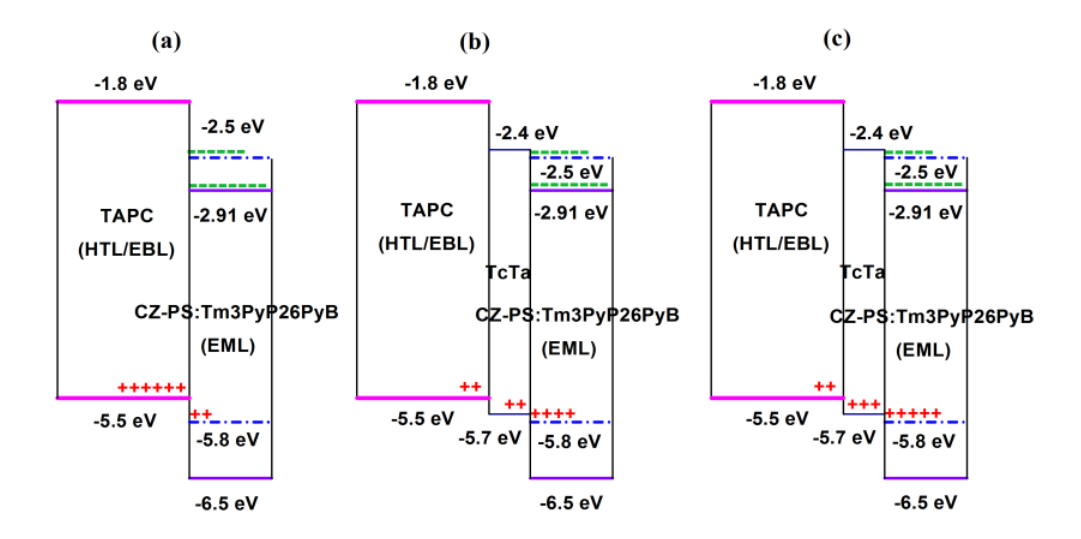


Fig. 8 Carriers' distribution in device (a), (b) and (c).

4. Conclusion

In summary, by doping CZ-PS in Tm3PyP26PyB, we successfully synthesized a high-efficiency dark blue EL device, which was widely used as ETL material, thus simplifying the device structure. 3 nm TCTA thin film between HTL and EML to balance the distribution of holes and electrons. Compared to previously reported results, the dark blue EL device has a low switch-on voltage of 2.8 V and a maximum brightness of 3914 cd/m². Finally, the maximum current efficiency, power efficiency and EQE of the optimized dark blue EL device were 12.58 cd/A, 12.69 lm/W and 13.1%, respectively. The CIE values were (0.176 and 0.159, respectively). At a brightness of 1000 cd/m², the current efficiency and the EQE of the device are 11.17 cd/A and 11.4%, respectively.

Declaration of Conflicting Interests

The author(s) declared no potential conflicts of interest with respect to the research, author-ship, and/or publication of this article.

Data Sharing Agreement

The datasets used and/or analyzed during the current study are available from the corresponding author on reasonable request.

Funding

The authors acknowledge the key Research Project of Henan Provincial Department of Education (25B510001).

References

- [1] S. Reineke, F. Lindner, G. Schwartz, N. Seidler, K. Walzer, B. Lüssem, K. Leo, White organic light-emitting diodes with fluorescent tube efficiency, Nature 459 (2009), 234–238. https://doi.org/10.1038/nature08003.
- [2] Y. Liu, C. Li, Z. Ren, S. Yan, M.R. Bryce, All-organic thermally activated delayed fluorescence materials for organic light-emitting diodes, Nat Rev Mater 3 (2018) 18020. https://doi.org/10.1038/natrevmats.2018.20.
- [3] N. Savage, Tomorrow's industries: from OLEDs to nanomaterials, Nature (2019). https://doi.org/10.1038/d41586-019-03764-1.
- [4] W.-J. Joo, J. Kyoung, M. Esfandyarpour, S.-H. Lee, H. Koo, S. Song, Y.-N. Kwon, S.H. Song, J.C. Bae, A. Jo, M.-J. Kwon, S.H. Han, S.-H. Kim, S. Hwang, M.L. Brongersma, Metasurface-driven OLED displays beyond 10,000 pixels per inch, Science 370 (2020) 6515. https://doi.org/10.1126/science.abc8530.
- [5] G. Pacchioni, OLEDs: Light my firefly, Nat Rev Mater 1 (2016) 18030. https://doi.org/10.1038/natrevmats.2016.30.
- [6] M. Hack, M. Lu, R. Kwong, M.S. Weaver, J.J. Brown, J.A. Nichols, T.N. Jackson, High-efficiency phosphorescent

- OLED technology, J Soc Inf Disp 11 (2003) 297-301. https://doi.org/10.1889/1.1825659.
- [7] W.S. Jeon, T.J. Park, S.Y. Kim, R. Pode, J. Jang, J.H. Kwon, Ideal host and guest system in phosphorescent OLEDs, Org Electron 10 (2008) 240-246. https://doi.org/10.1016/j.orgel.2008.11.012.
- [8] M. Flämmich, J. Frischeisen, D.S. Setz, D. Michaelis, B.C. Krummacher, T.D. Schmidt, W. Brütting, N. Danz, Oriented phosphorescent emitters boost OLED efficiency, Org Electron 12 (2011) 1663-1668. https://doi.org/10.1016/j.orgel.2011.06.011.
- [9] D. Jacquemin, D. Escudero, The short device lifetimes of blue PhOLEDs: insights into the photostability of blue Ir(III) complexes, Chem Sci 8 (2017) 7884-7850. https://doi.org/10.1039/c7sc03905k.
- [10] A. Saeed, M. Faisal, F.A. Larik, H.R. El-Seedi, P.A. Channar, D. Shahzad, Recent Progress in Pyridine Containing Heterocycles as High Performance Host Materials for Blue PHOLEDs, Mini Rev Org Chem 15 (2018) 261-273. https://doi.org/10.2174/1570193x15666171227162050.
- [11] F. Rizzo, F. Cucinotta, Recent Developments in AIEgens for Non-doped and TADF OLEDs, Isr J Chem 58 (2018) 874-888. https://doi.org/10.1002/ijch.201800049.
- [12] G. Grybauskaite-Kaminskiene, K. Ivaniuk, G. Bagdziunas, P. Turyk, P. Stakhira, G. Baryshnikov, D. Volyniuk, V. Cherpak, B. Minaev, Z. Hotra, H. Ågren, J.V. Grazulevicius, Contribution of TADF and exciplex emission for efficient "warm-white" OLEDs†, J Mater Chem C Mater 6 (2018) 1543-1550. https://doi.org/10.1039/c7tc05392d.
- [13] O. Bezvikonnyi, D. Gudeika, D. Volyniuk, A. Bucinskas, J. V Grazulevicius, Derivatives of triphenyltriazine and ditert-butylcarbazole as TADF emitters for sky-blue OLEDs, Materials Science and Engineering: B (2021) 115441. https://doi.org/10.1016/j.mseb.2021.115441.
- [14] Y. Xiao, H. Wang, Z. Xie, M. Shen, R. Huang, Y. Miao, G. Liu, T. Yu, W. Huang, NIR TADF emitters and OLEDs: challenges, progress, and perspectives, Chem Sci (2022) 13, 8906-8923. https://doi.org/10.1039/d2sc02201j.
- [15] E. V Puttock, C.S.K. Ranasinghe, M. Babazadeh, J. Jang, D.M. Huang, Y. Tsuchiya, C. Adachi, P.L. Burn, P.E. Shaw, Solution-Processed Dendrimer-Based TADF Materials for Deep-Red OLEDs, Macromolecules 53 (2020), 10375–10385. https://doi.org/10.1021/acs.macromol.0c02235.
- [16] J.-M. Teng, Y.-F. Wang, C.-F. Chen, Recent progress of narrowband TADF emitters and their applications in OLEDs, J Mater Chem C Mater 8 (2020) 11340-11353. https://doi.org/10.1039/d0tc02682d.
- [17] H. Uoyama, K. Goushi, K. Shizu, H. Nomura, C. Adachi, Highly efficient organic light-emitting diodes from delayed fluorescence, Nature 492 (2012) 234–238. https://doi.org/10.1038/nature11687.
- [18] T. Zhang, B. Zhao, B. Chu, W. Li, Z. Su, X. Yan, C. Liu, H. Wu, F. Jin, Y. Gao, Efficient exciplex emission from intramolecular charge transfer material, Org Electron 25 (2015) 6-11. https://doi.org/10.1016/j.orgel.2015.06.017.
- [19] M. Kim, S.K. Jeon, S. Hwang, J.Y. Lee, Stable Blue Thermally Activated Delayed Fluorescent Organic Light-Emitting Diodes with Three Times Longer Lifetime than Phosphorescent Organic Light-Emitting Diodes, Advanced Materials 27 (2015) 2515–2520. https://doi.org/10.1002/adma.201500267.
- [20] T.-Y. Kim, D.-G. Moon, Electrical and Optical Properties of Phosphorescent Organic Light-Emitting Devices with a TAPC Host, Transactions on Electrical and Electronic Materials 12 (2011) 84-87. https://doi.org/10.4313/teem.2011.12.2.84.
- [21] Y. Dai, H. Zhang, Z. Zhang, Y. Liu, J. Chen, D. Ma, Highly efficient and stable tandem organic light-emitting devices based on HAT-CN/HAT-CN:TAPC/TAPC as a charge generation layer, J Mater Chem C Mater 3 (2015) 6809-6814. https://doi.org/10.1039/c4tc02875a.
- [22] W. Stampor, Electromodulation of fluorescence in hole-transporting materials (TPD, TAPC) for organic light-emitting diodes, Chem Phys 265 (2000) 361-362. https://doi.org/10.1016/s0301-0104(00)00123-3.
- [23] Q. Zhang, J. Li, K. Shizu, S. Huang, S. Hirata, H. Miyazaki, C. Adachi, Design of Efficient Thermally Activated Delayed Fluorescence Materials for Pure Blue Organic Light Emitting Diodes, J Am Chem Soc 134 (2012) 14706–14709. https://doi.org/10.1021/ja306538w.
- [24] Q. Zhu, L. Zhou, R. Wu, Z. Li, R. Cui, X. Zhao, Q. Duanmu, High efficiency white organic light-emitting diodes with co-doped iridium complexes as blue and yellow emitters, Synth Met 272 (2021) 116666. https://doi.org/10.1016/j.synthmet.2020.116666.
- [25] X. Zhao, L. Zhou, Q. Zhu, R. Cui, Y. Cui, W. Liu, J. Wang, X. Mi, Efficient red electroluminescent devices with very low operation voltage by utilizing hole and electron transport materials as the host, Thin Solid Films 717 (2021) 138474. https://doi.org/10.1016/j.tsf.2020.138474.

- [26] Y. Sun, W. Sun, D. Zhang, J. Yin, M. Mao, L. Zhou, Deep-Red Organic Light-Emitting Diodes with Increased External Quantum Efficiency and Extended Operational Lifetime by Managing the Composition of Mixed Cohosts, The Journal of Physical Chemistry C 127 (2023) 19378-19385. https://doi.org/10.1021/acs.jpcc.3c04174.
- [27] J.-H. Jou, J.-R. Tseng, K.-Y. Tseng, W.-B. Wang, Y.-C. Jou, S.-M. Shen, Y.-L. Chen, W.-Y. Hung, S.-Z. Chen, T. Ding, H.-C. Wang, High-efficiency host free deep-blue organic light-emitting diode with double carrier regulating layers, Org Electron 13 (2012) 2893-2897. https://doi.org/10.1016/j.orgel.2012.08.040.
- [28] J. Vollbrecht, Excimers in organic electronics, New Journal of Chemistry 42 (2018) 11249-11254. https://doi.org/10.1039/c8nj02135j.
- [29] B.T. Diroll, W. Cho, I. Coropceanu, S.M. Harvey, A. Brumberg, N. Holtgrewe, S.A. Crooker, M.R. Wasielewski, V.B. Prakapenka, D. V Talapin, R.D. Schaller, Semiconductor Nanoplatelet Excimers, Nano Lett 18 (2018) 6948–6953. https://doi.org/10.1021/acs.nanolett.8b02865.
- [30] R. Zhao, C. Hettich, J. Zhang, M. Liu, J. Gao, Excimer Energies, J Phys Chem Lett 14 (2023) 2917–2926. https://doi.org/10.1021/acs.jpclett.3c00545.